Journal of Modern Optics
Vol. 53, Nos. 16–17, 10–20 November 2006, 2303–2308

Taylor & Francis
Taylor & Francis Group

Photonic crystal vertical cavity surface emitting laser arrays

ANN C. LEHMAN†, JAMES J. RAFTERY JR‡ and
KENT D. CHOQUETTE*†

†Micro and Nanotechnology Laboratory, Department of Electrical and Computer Engineering, University of Illinois at Urbana-Champaign, Urbana, Illinois 61801, USA
‡US Military Academy at West Point, NY, USA

(*Received 13 February 2006*)

Coherent coupling of 2×1 photonic crystal (PhC) vertical cavity surface emitting laser (VCSEL) arrays is studied. It is found that the relative phase between lasing defects, also known as the phase angle of the complex degree of coherence, varies with injection current. The amplitude of the complex degree of coherence also depends on current. Additionally, it is shown that the magnitude of the complex degree of coherence between defects is maximized near in-phase and out-of-phase conditions.

1. Introduction

Arrays of microcavity laser diodes provide potential solutions for applications such as optical storage, optical imaging and beam-steering. Evanescent optical coupling between 2-dimensional (2D) array elements of vertical cavity surface emitting lasers (VCSELs) has been studied extensively [1–7]. One of the major disadvantages with this coupling approach is that the large inherent loss between cavities typically causes the laser phases to lock together out-of-phase [1]. That is to say, the emission from one cavity is 180° out-of-phase with emission from a neighbouring cavity, which results in a far-field emission pattern with an on-axis null. For most applications, one would prefer that the coupled lasers emit with the same phase to produce an in-phase far field profile with an on-axis central lobe or have a controllable variable phase difference which would produce electronic beam-steering. Antiguided VCSELs [8, 9] and phase-adjusted arrays [5] have been studied as an alternative approach to achieve in-phase coupling, but these arrays are complicated to fabricate and have stringent design tolerances.

Photonic crystal (PhC) VCSELs are created when a periodic pattern of holes is etched into the surface of a VCSEL. Defects are created by removing holes from the pattern, and lasing is confined within these regions. This study examines 2×1 coherently coupled VCSEL arrays. An example of a near field image and a schematic

*Corresponding author. Email: choquett@uiuc.edu

Journal of Modern Optics
ISSN 0950–0340 print/ISSN 1362–3044 online
http://www.tandf.co.uk/journals
DOI: 10.1080/09500340600894030

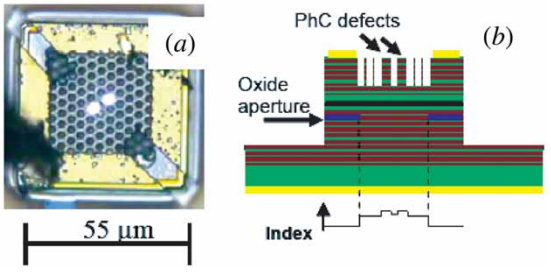

Figure 1. (*a*) Top view of lasing PhC VCSEL array with segmented electrical contacts. (*b*) Cross-sectional schematic of PhC VCSEL and a depiction of the refractive index profile.

showing the cross-sectional view of a device with two defects are shown in figure 1. The hole between the defects may be varied in diameter and etch depth allowing control of the refractive index between defects. By design of the dimensions of this hole, the coupling between defects can be controlled [6].

For the devices studied, a standard VCSEL process was used to fabricate devices emitting at nominally 850 nm. The VCSELs had 25 top periods and 35 bottom periods in their distributed Bragg reflector mirrors. Following the fabrication, a half-wavelength of oxide was left on the top facet for a focused ion beam etch (FIBE) process step. A pattern with a triangular lattice similar to that shown in figure 1 was etched through the top layer of oxide. The patterned oxide was used as a mask to transfer the PhC pattern into the top facet of the VCSELs using an inductively coupled reactive ion etch. The photonic crystal pattern consisted of hexagonally arranged holes separated by 4 μm with a value of 0.6 or 0.7 for the ratio of hole diameter to lattice spacing. The diameter of the centre hole between the defects was varied between 1.2 to 2.2 μm.

2. Relative phase angle

As discussed in [7], the relative phase between the cavities may be determined from the far-field emission pattern. This quantity is also known as the phase of the complex degree of coherence as discussed in [10]. Using basic antenna array theory, the beam pattern may be separated into the element pattern multiplied by the array factor. The array factor would be the resultant beam pattern in the event of isotropic point sources. Following [11], the array factor is given by the form:

$$|\mathrm{ARFAC}(\psi)| = \left|\frac{\sin(N\psi/2)}{\sin(\psi/2)}\right|, \tag{1}$$

where N is the number of elements in the array. ψ is given by

$$\psi = kd\cos\theta + \delta, \tag{2}$$

where $k = 2\pi n/\lambda$ is the wavevector, n is the index of refraction, λ is the emission wavelength in free space, d is the distance between emission centres, θ is the angle measured from parallel to the VCSEL facet along the axis containing the defects, and δ is the relative phase difference between adjacent emitters. When δ is zero (in-phase), a main on-axis lobe is emitted in the direction perpendicular to the surface of the VCSEL. As δ is varied away from zero, the angle of emission for that lobe moves away from perpendicular along the axis containing the line of array elements. The out-of-phase case ($\delta = 180^\circ$) produces two nominally equal lobes with an on-axis null. It is also important to remember that only lobes falling within the emission pattern of a single element will radiate. In our case, we use a Gaussian envelope to approximate the diffraction limited radiation from each defect cavity. This envelope explains why even for a relatively large kd value of approximately 51 rad, we do not observe more than two main lobes.

A series of PhC VCSELs were tested under continuous wave (CW) and pulsed operation at room temperature. During operation, the near-field pattern of these devices indicates lasing is confined to the two defect regions. Examples of the far-field profile for increasing bias currents are shown in figure 2. As the electrical bias to the VCSEL varies, the peaks in the far-field patterns change in relative intensity and shift in angle. Between 25 and 60 mA, the right peak reduces in relative amplitude and moves by 1.60°, and the left peak increases in amplitude and shifts by 1.37°. This shift in emission angle is characteristic of a relative phase change between the two defect regions and can be determined using equation (1).

Using the formulation given above along with the locations of the minima in the patterns, the relative phase difference was calculated as a function of injection current. From the theory, we find that the relative amplitude in each defect cavity will affect the magnitude of the minima but not the location of the minima with respect to phase. A plot of the phase difference between the cavities versus current is shown in figure 3. As the dc current varied from 34 to 58 mA, the phase difference between the defects varied from 203° to 122°. Thus for this coupled array, the relative phases varied about the out-of-phase condition.

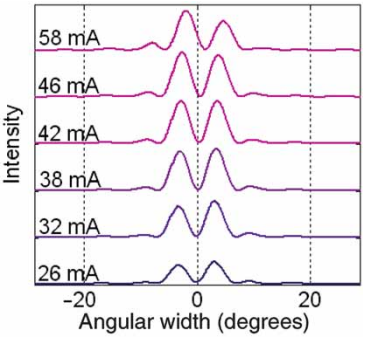

Figure 2. Offset far-field profiles at injection currents of 26, 32, 38, 42, 46 and 58 mA. (The colour version of this figure is included in the online version of the journal.)

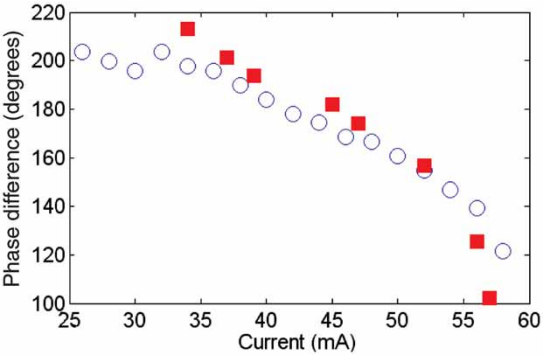

Figure 3. Relative phase difference between cavities at various CW (◯) and pulsed (□) current biases. (The colour version of this figure is included in the online version of the journal.)

The relative changes in phase may be caused by thermal or electronic effects on the refractive index. In order to examine the effects of heating, far-field measurements were also taken under pulsed injection conditions (1 μs with a 50% duty cycle). The phase tuning effect under pulsed operation, also plotted in figure 3, is nearly identical to that observed under continuous wave operation. This suggests that thermal effects are not a main contributor to the phase variation because the phase tuning did not decrease. Another contribution to the refractive index in the VCSEL cavities arises from the injected electrons. Thus the suppression of the refractive index in the lasing regions as carrier density increases along with a varying current distribution between the cavities likely plays a role in how the cavities are phase-locked.

3. Array coherence

One may also use the far-field patterns to examine the degree of coherence between defects. As discussed by Mandel and Wolf for Young's two pinhole experiment [10], which is similar to our 2×1 array if each defect is considered as a pinhole, the visibility of an interference pattern may be found by

$$V = \frac{\langle I \rangle_{\max} - \langle I \rangle_{\min}}{\langle I \rangle_{\max} + \langle I \rangle_{\min}}, \tag{3}$$

where $\langle I \rangle_{\max}$ is the averaged maximum intensity and $\langle I \rangle_{\min}$ is the averaged minimum intensity in the interference pattern. Also, for a stationary, ergodic field with two elements the visibility is related to the coherence by

$$V = \frac{2}{(I_1/I_2)^{1/2} + (I_2/I_1)^{1/2}} |\gamma|. \tag{4}$$

where γ is the complex degree of coherence between adjacent devices and I_j is the near-field intensity of the jth element. The complex degree of coherence is a measure of how correlated fluctuations in the field emitted from one defect are with the fluctuations in the field emitted from the other defect. Therefore, the magnitude of the complex degree of coherence between two defects in a photonic crystal may be found from the visibility of the far-field patterns as well as near-field measurements of the relative intensities between defects. However, our 2×1 array is similar but not completely equivalent to Young's two-pinhole experiment. Since each laser in the array emits a Gaussian beam, a Gaussian is de-convolved from the far-field interference fringes to accurately measure the visibility.

From far-field data, near-field data, and equations (3) and (4), we have measured the visibility and the magnitude of the complex coherence as a function of current. We find that the visibility and complex degree of coherence are nearly identical since there is very little variation between the intensity of each defect region. On one hand, this is not surprising, given the defects are separated by less than 4 μm, and the current injection is nominally uniform. However, as evident by figures 2 and 3, there is sufficient difference of carriers to induce a phase difference between cavities. Future experiments will examine the effects of separating the electrical contact to each defect to create an intentional current injection asymmetry.

In figure 4 we plot the visibility versus relative phase between elements as current is varied to the array. From this plot it is clear that as current changes, the relative phase between adjacent defects also changes, and the visibility/coherence is

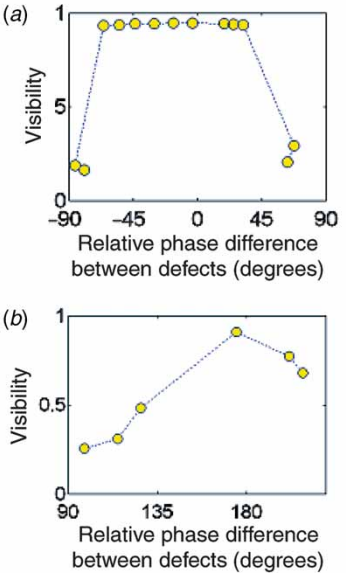

Figure 4. (*a*) Visibility as a function of the relative phase between cavities for an in-phase device. (*b*) Visibility as a function of relative phase between cavities for an out-of-phase device fabricated with the same material as in (*a*). (The colour version of this figure is included in the online version of the journal.)

correlated with the phase. As the phase difference nears 0° or 180° (in- or out-of-phase), the coherence approaches unity. As the phase deviates from 0° or 180°, the coherence decreases. Hence, in- or out-of-phase operation exhibits the greatest coherence, whereas when there is a 'phase slip' between the defect cavities, the coherence degrades.

4. Conclusion

In conclusion, both the phase and amplitude of the complex degree of coherence have been studied for 2×1 arrays of PhC VCSELs. It has been observed that both are functions of injection current to the array. Also, it has been found that the visibility, which essentially equals the amplitude of the degree of coherence, is maximized near in-phase and out-of-phase conditions. The change in phase angle may allow for beam-steering applications although this will be limited by the drop in coherence.

Acknowledgment

This work was supported by the National Science Foundation under Grant No. 0121662

References

[1] G.R. Hadley, Opt. Lett. **15** 1215 (1990).
[2] H.-J. Yoo, J.R. Hayes, E.G. Paek, *et al.*, IEEE J. Quantum Electron. **26** 1039 (1990).
[3] P.L. Gourley, M.E. Warren, G.R. Hadley, *et al.*, Appl. Phys. Lett. **58** 890 (1991).
[4] M. Orenstein, E. Kapon, J. P. Harbison, *et al.*, Appl. Phys. Lett. **60** 1535 (1992).
[5] M.E. Warren, P.L. Gourley, G.R. Hadley, *et al.*, Appl. Phys. Lett. **61** 1484 (1992).
[6] A.J. Danner, J.C. Lee, J.J. Raftery Jr, *et al.*, Electron. Lett. **39** 1323 (2003).
[7] A.C. Lehman, J.J. Raftery Jr, A.J. Danner, *et al.*, Appl. Phys. Lett. **88** 021102 (2006).
[8] D.K. Serkland, K.D. Choquette, G.R. Hadley, *et al.*, Appl. Phys. Lett. **75** 3754 (1999).
[9] R. Monti di Sopra, M. Brunner, H.-P. Gauggel, *et al.*, Appl. Phys. Lett. **77** 2283 (2000).
[10] L. Mandel and E. Wolf, *Optical Coherence and Quantum Optics* (Cambridge University Press, New York, 1995).
[11] See a microwave antenna theory text for example, M.T. Ma, *Theory and Application of Antenna Arrays* (Wiley, New York, 1974).